Indian J Phys
DOI 10.1007/s12648-012-0070-x

ORIGINAL PAPER

VLF signals in summer and winter in the Indian sub-continent using multi-station campaigns

S K Chakrabarti[1,2]*, S K Mondal[2], S Sasmal[2], S Pal[1], T Basak[1], S Chakrabarti[2], D Bhowmick[2], S Ray[2], S K Maji[2], A Nandi[2], V K Yadav[2], T B Kotoch[2], B Khadka[2], K Giri[1], S K Garain[1], A K Choudhury[2], N N Partra[3] and N Iqbal[4]

[1]SN Bose National Centre for Basic Sciences, JD-Block, Salt Lake, Kolkata 700 098, India

[2]Indian Centre for Space Physics, 43 Chalantika, Garia Station Road, Kolkata 700 084, India

[3]NCRA/TIFR, Ganeshkhind, Pune 411 007, Maharashtra, India

[4]Department of Physics, University of Kashmir, Srinagar 190 003, India

Received: 06 May 2011 / Accepted: 01 September 2011

Abstract: We have carried out 2 week-long campaigns in Indian winter and summer to study VLF signals from the Indian navy transmitter (VTX) operating at 18.2 kHz. We have used more than a dozen of receivers scattered throughout the Indian sub-continent in each of these campaigns. To our knowledge, this is the largest campaign of its kind in this region. The propagation paths range from 500 km to almost 3,000 km covering an area of about 4 million sq km. We have presented the results of the amplitude variation of the diurnal signal at each of these receiving stations in winter and summer and compare them. We have clearly found the non-reciprocity of the east to west and west to east propagation. Our results generally agree with the signal shapes obtained using the long wave propagation capability code based on mode propagation through the Earth-ionosphere cavity.

Keywords: Radio waves; Waveguides; D-region; Ionosphere

PACS Nos.: 41.20.Jb; 84.40.Az; 94.20.de; 94.20.wq

1. Introduction

Having a very low frequency (VLF) radio wave transmitter right at the southern tip of India close to the geomagnetic equator and having a geomagnetic meridian ($\sim 150°$E) passing through the transmitter roughly dividing the land-mass into two equal parts, makes the Indian subcontinent an ideal test bed for the theoretical models of VLF signal propagation through the Earth-ionosphere waveguide propagation. A further advantage is that there is no complexity due to trans-equatorial propagation. The entire path is generally on the land mass and thus the effects of ground conductivity could be considered to be uniform for all the stations. While many studies of VLF signal propagation are present in the literature over last few decades in different parts of the world, in the context of the Indian sub-continent no extensive studies are made [1–4].

Indian Centre for Space Physics has been monitoring VLF radio waves for about a decade from a single station and reported observations related to Leonid meteor showers [1] and solar flares [2] before. However, observations from multiple stations have not been reported before. In this paper, we will exploit the unique geographical and geomagnetic properties mentioned above and present the results of the VLF signal amplitude variation simultaneously received at over a dozen of sites all over India and Nepal both in the summer and the winter. We specifically concentrate on the short distance (less than 3,000 km) propagation characteristics of the signal from the Indian Navy station VTX (at Vijayanarayanam: 08°23′N, 77°45′E) transmitting at 18.2 kHz. As stated above, because of the unique geomagnetic properties of the VTX station and the geographic location of the Indian sub-continent itself, it is possible for us to study the east–west and west–east propagation effects at short distances also during our

*Corresponding author, E-mail: chakraba@bose.res.in

Published online: 26 May 2012

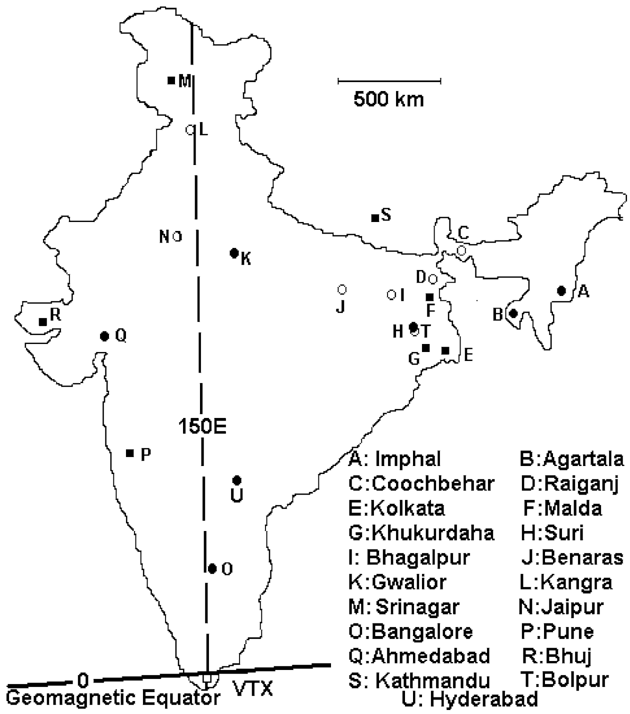

Fig. 1 The map of India showing all the receiving stations employed in our campaigns. Those stations participating in the summer and winter campaigns are plotted with *open circles* and *filled circles*, while those by *filled squared boxes* are common to both the campaigns. The geomagnetic equator and the magnetic longitude passing close to the VTX transmitter station are plotted for reference

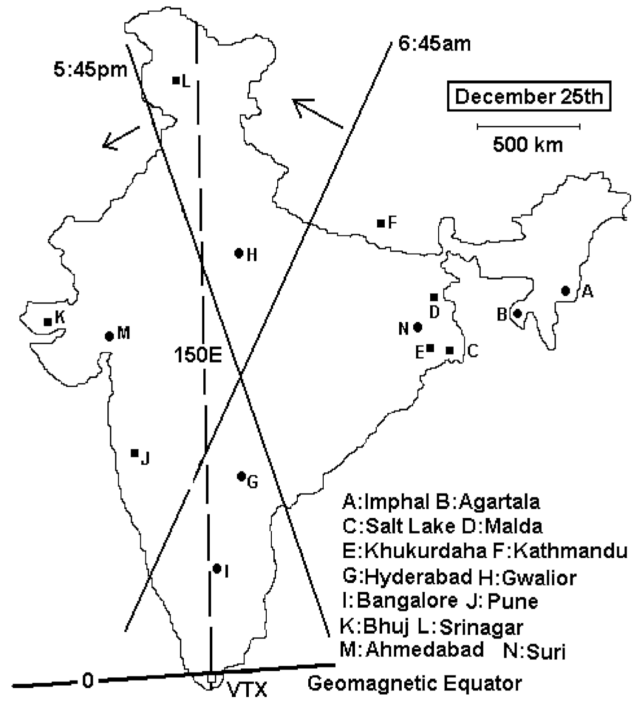

Fig. 2 The map of India showing all the receiving stations employed in our winter campaigns. Those shown by *filled squared boxes* are common to both summer and winter campaigns while those with *filled circles* are only for winter campaigns. The geomagnetic equator and the magnetic longitude passing close to the VTX transmitter station are plotted for reference. The sunrise terminator and the sunset terminator at 6:30 am and 6:00 pm are shown to suggest how the signals would be influenced by the passage of the inclined terminators

campaign. Furthermore, using this campaign, we now have a clear idea of what types of signals to expect from different parts of this vast sub-continent.

There are several works of VLF wave propagation through the Earth-ionosphere waveguide using the wave-hop theory [5, 6] and several works which compute the signal strength using the wave-mode theory [7, 8]. It is generally believed that at VLF frequencies wave-hop and waveguide theory are complimentary. The number of wave-hops which needs to be taken into account reduces as VLF paths shorten whereas the number of waveguide modes increases. However, every propagation path has its own characteristics as it may be partly on land and partly on sea or totally on land or sea. Thus, it is very difficult to understand the signal characteristics using simple minded models which exist in the literature. The most well-known code called the long wave propagation capability (LWPC) [9], predicts an average behavior of the reflection height and the exponential sharpness factor (β) of electron distribution [10]. This code works generally well, though the result does not automatically give details of a narrow-band profile over the whole day. An interesting early observation was that the signal amplitude did not appear to be reciprocal in the easterly and westerly directions [11]. This is promptly explained by generally south to north orientation of the magnetic field lines [12–14]. LWPC calculations usually reproduce the observed asymmetry.

Table 1 Winter campaign stations

Place	Latitude and longitude	Distance (km)	Sunrise (IST)	Sunset (IST)
Imphal	24°44′N, 93°58′E	2,503	05:56	16:33
Agartala	23°50′N, 91°15′E	2,434	05:54	16:34
Salt Lake	22°34′N, 88°24′E	1,963	06:14	17:00
Malda	25°00′N, 88°09′E	2,166	06:20	16:55
Khukurdaha	22°27′N, 87°45′E	1,894	06:16	17:02
Kathmandu	27°45′N, 85°20′E	2,296	06:37	17:01
Hyderabad	17°20′N, 78°30′E	998	06:43	17:49
Gwalior	26°14′N, 78°10′E	1,985	07:02	17:33
Bangalore	12°58′N, 77°38′E	509	06:39	18:01
Pune	18°34′N, 73°49′E	1,183	07:04	18:05
Bhuj	23°14′N, 69°40′E	1,863	07:30	18:13
Srinagar	34°08′N, 74°51′E	2,867	07:34	17:27
Suri	23°54′N, 87°32′E	2,015	06:20	17:00
Ahmedabad	23°03′N, 72°40′E	1,701	07:18	18:01

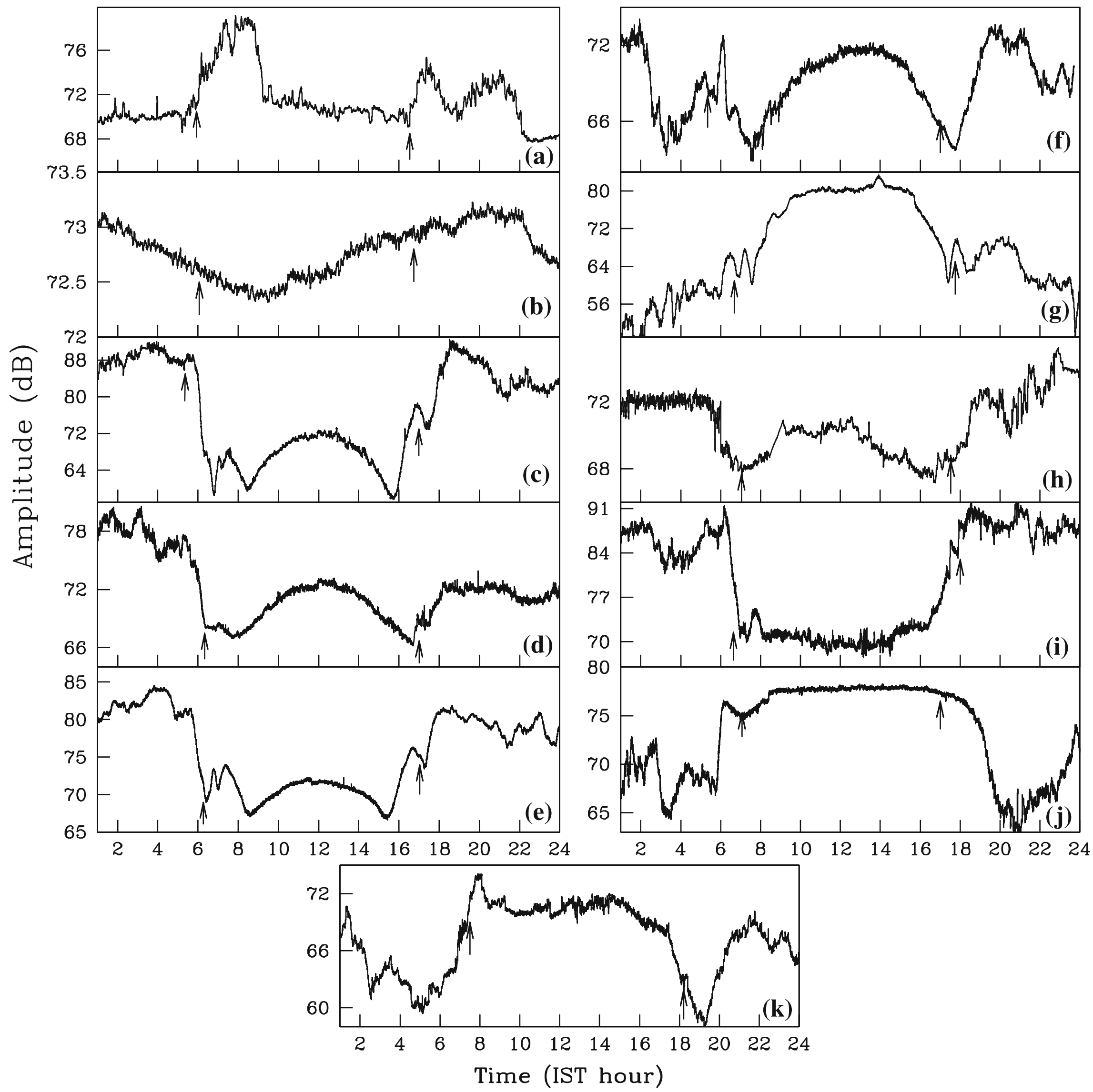

Fig. 3 Normalized observed data over the whole day in Indian Standard Time (IST = UT + 5:30 h) from some of the receiving stations in winter: (*a*) Imphal, (*b*) Agartala, (*c*) Salt Lake, (*d*) Malda, (*e*) Khukurdaha, (*f*) Kathmandu, (*g*) Hyderabad, (*h*) Gwalior, (*i*) Bangalore, (*j*) Pune, and (*k*) Bhuj. The data at (*c*–*f*) and (*h*) have strong night and weak daytime signals. The data at (*g*), (*j* and *k*) have strong day time and weak night time signals. The data at Bangalore (*i*) is dominated by ground wave in the daytime. The data at (*a* and *b*) are not easy to understand

One of the objectives of our campaigns is to calibrate the actual observations as a function of geographical location. It is thought that the ionosphere is affected by seismic activities [15, 16] which may be taking place far away and in order to quantify such effects, one requires to calibrate the entire signal pattern on non-seismic days. It is expected that the seismic effects would depend on the proximity of the seismic centers from the propagation paths from the transmitter to the receiver. Thus, in principle one could 'zero-in' on the possible seismic centers from the observations of anomalous signals from a large number of receivers. Another objective is to use the Earth's ionosphere as a gigantic detector of high energy phenomena. Thus we can study how the detector functions, i.e., how the ionosphere is globally affected by extra-terrestrial events, such as the solar flares or very high energetic processes such as the gamma-ray bursts (GRBs), soft-gamma ray (SGR) repeaters, etc. [17, 18]. Similarly, a number of stations provide us with the ionospheric weather conditions. In future, we will increase the number of permanent stations for such studies. Our present campaigns may be thought of as 'dry-runs' for such permanent stations which could be required for disaster managements and for detection of high energy phenomena in space.

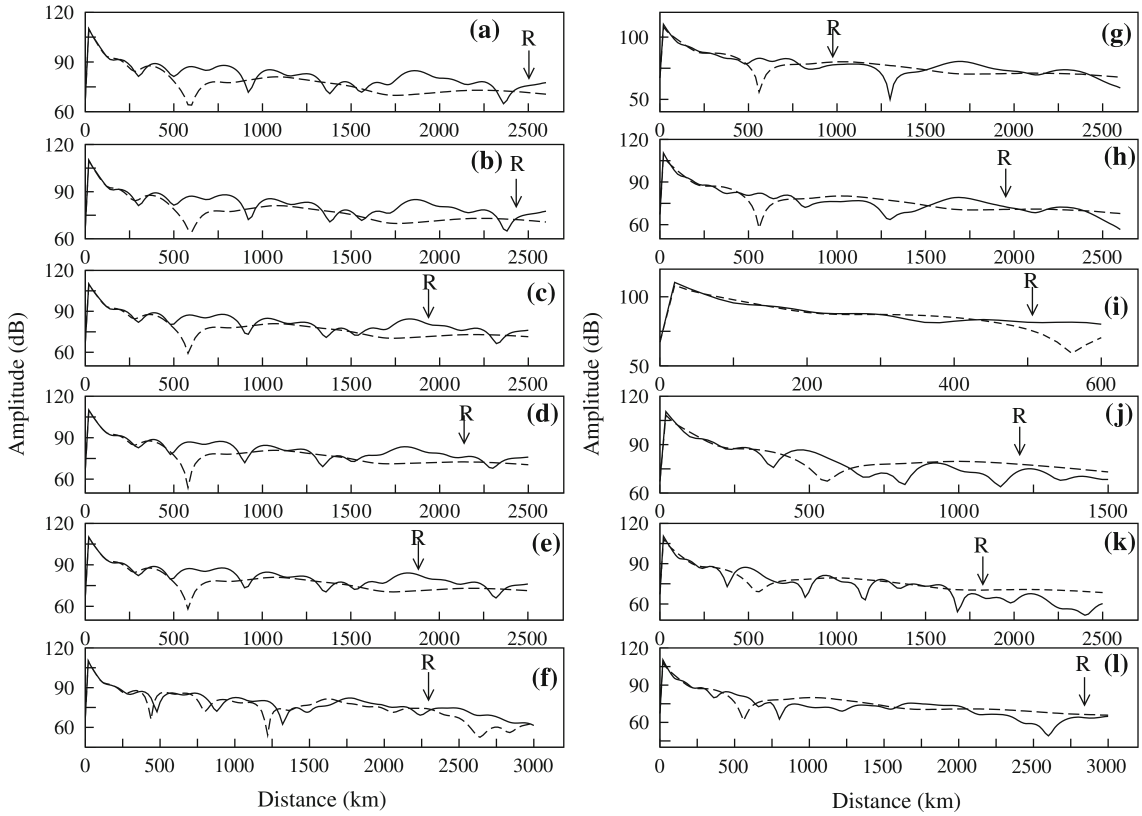

Fig. 4 The variation of the VLF signal amplitude as a function of the distance between the transmitter and the receiver as obtained from LWPC. For plotting purpose, we assume the day to be 27th December in the winter campaign. R marks is the position of the receiver. The signals are for (*a*) Imphal, (*b*) Agartala, (*c*) Salt Lake, (*d*) Malda, (*e*) Khukurdaha, (*f*) Kathmandu, (*g*) Hyderabad, (*h*) Gwalior, (*i*) Bangalore, (*j*) Pune, (*k*) Bhuj, and (*l*) Srinagar. The *curves* are drawn at 00:00:00 IST (*solid*) and 12:00:00 IST (*dashed*), respectively

In the next section, we discuss the properties of the instruments and antennas used in our campaign. In Sect. 3, we discuss the results in the winter campaign. In Sect. 4, we present and discuss the results in the summer campaign. In Sect. 6, we compare our results and present interpretations based on the LWPC simulations. Finally, in Sect. 5, we make concluding remarks.

2. The receiver, antenna, and the campaign locations

In the campaigns the data were received at 14 stations in summer and winter, though only seven stations were common to both the campaigns. The places were chosen in a way that the entire Indian sub-continent may be covered, though there were more receiving stations in the eastern region due to the proximity with respect to the Indian centre for Space Physics. We used square-shaped loop antennas (3.5 × 3.5 ft) having 17 No. of turns of 1 sq mm PVC flexible wire having 3.2 Ohm resistance and 2 mH inductance. The receiver is of Gyrator-III type with a band pass filter having the range of 5–30 kHz. The planes of the loop antenna at each location directed towards the transmitter in order to maximize the sensitivity. The signal from the antenna was fed to the line receiver and the output from the receiver, after suitable amplification, was fed into the audio input of the computers. The signals were automatically recorded and stored, twice a second. The results from all the receivers were brought in at the head quarter and for analysis and comparison.

Figure 1 reproduces the schematic boundary of India. The transmitter (VTX) is shown as an open box. All the receiving stations are indicated as the filled squared box (where both summer and winter campaigns were held), filled circles (where only the winter campaigns were held) and open circles (where only the summer campaigns were held). The same conventions will be used for Figs. 2, 6 also. The geomagnetic equator runs roughly east to west, and passes within less than a degree north of the VTX transmitter. The 150°E geomagnetic meridian (referred to as the central geomagnetic meridian or CGM in the rest of this paper) which passes through the transmitter roughly divides India into two halves. To see the non-reciprocity of the East–West propagation effects, we placed the stations on both sides of this central meridian in each of the campaigns. A region around a fixed-

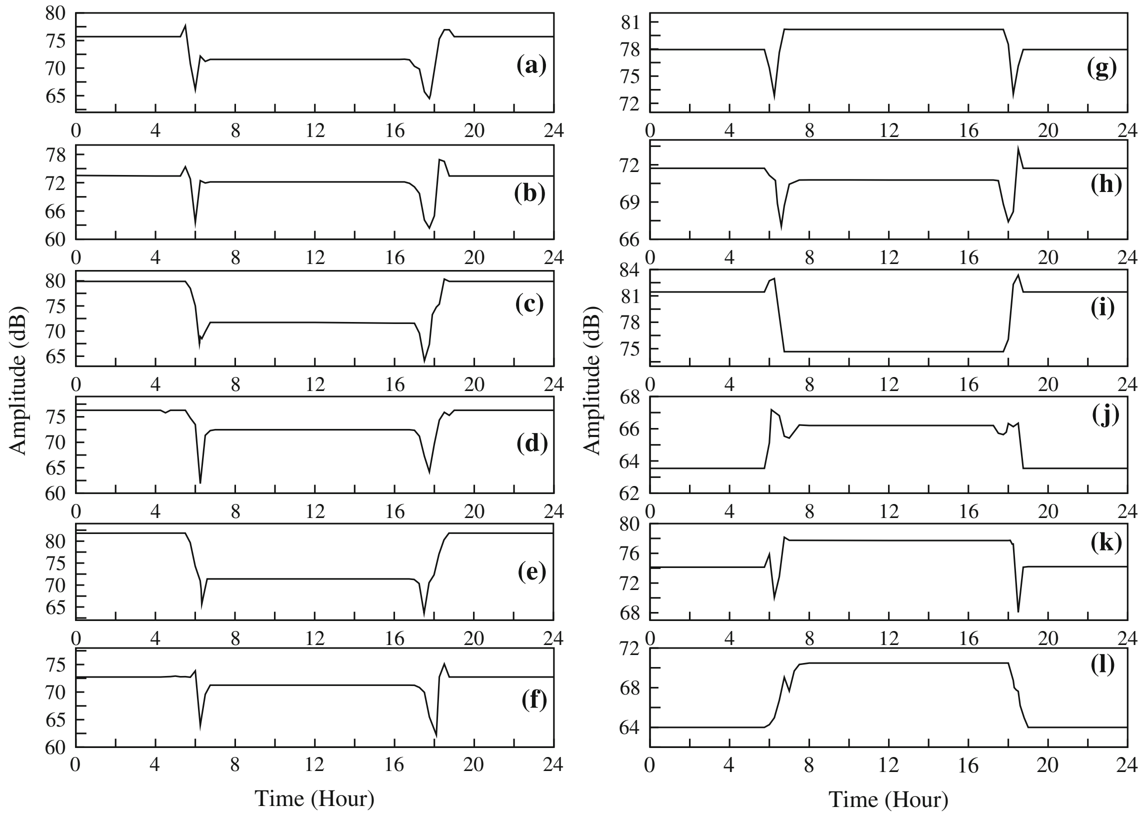

Fig. 5 The diurnal variation of the VLF signal amplitude at different receiving stations as obtained by LWPC in winter. The signals are for (*a*) Imphal, (*b*) Agartala, (*c*) Salt Lake, (*d*) Malda, (*e*) Khukurdaha, (*f*) Kathmandu, (*g*) Hyderabad, (*h*) Gwalior, (*i*) Bangalore, (*j*) Pune, (*k*) Bhuj, and (*l*) Srinagar. The results generally match with observations qualitatively, though the details are missing

frequency transmitter is not likely to receive the ground wave or a sky wave, and is called a skip zone. We kept a receiver at Bangalore just near the skip distance at VTX frequency. We also had a receiver placed at Kathmandu, Nepal which received data in both the seasons. We identified the average observed signal at the noon with the computed LWPC signal for each of the receivers. This would normalize the data with a standard yardstick and would be easier to compare.

3. Results from the winter campaign and interpretation

The campaign was conducted from the 21st to 31st of December, 2008. Table 1 shows the locations of the stations and their distances along the great circle path (GCP) from the transmitter. We also provide the sunrise and sunset times for reference purpose. In Fig. 2, we show schematically the locations of the receiving stations in the winter campaigns. Out of the 14 stations, ten were in the east and four were in the west of CGM. We present the sunrise and sunset terminators on a typical day of the campaign at 6.45 am and 5.45 pm, respectively. Their directions of movements are shown with arrows. In Fig. 3, we present the received signals. The station are at (a) Imphal, (b) Agartala, (c) Salt Lake, (d) Malda, (e) Khukurdaha, (f) Kathmandu, (g) Hyderabad, (h) Gwalior, (i) Bangalore, (j) Pune, and (k) Bhuj (See also Fig. 2 for corresponding station locations on the map).

We observe that, roughly speaking, there are two types of signals: The signals of (c–f) and (h–i) belong to 'Eastern' type or E-type, where the night time signals are stronger and the daytime signals are weak. Also, the day time signal clearly follows the zenithal flux variation of the Sun. The other type is 'Western' type or W-type. The signals of (g) and (j and k) belong to this group where the day time signal is strong, the night time signal is strongly attenuated, and the daytime signal is flatter than what is expected from the diurnal solar flux variation. The signal at (i) is unusually flat in the day time while at night it is strong and variable, similar to the other measurements. The signals at (a and b) are peculiar and do not show the sunrise/sunset terminators very well. The signal at Agartala (b) is very flat, only about 1 dB variation in 24 h. The arrows in

Table 2 Signal amplitudes and average attenuation rates from LWPC

Place	Signal (dB) noon and night 06:30 UT, 18:30 UT	Noon 1st and 2nd modes (dB Mm^{-1})	Midnight 1st and 2nd modes (dB Mm^{-1})
(A) Imphal	71.5, 75.7	2.57, 5.81	0.731, 2.51
(B) Agartala	72.8, 77.3	2.57, 5.79	0.73, 2.51
(C) Coochbehar	71.82, 71.03	2.62, 5.89	0.76, 2.65
(D) Raiganj	72.26, 75.53	2.63, 5.93	0.76, 2.65
(E) Salt Lake	71.56, 80.42	2.60, 5.80	0.74, 2.63
(F) Malda	72.47, 76.29	2.62, 5.91	0.76, 2.65
(G) Khukurdaha	71.68, 80.00	2.60, 5.77	0.74, 2.68
(H) Suri	72.20, 78.20	3.22, 5.884	1.01, 2.71
(I) Bhagalpur	72.14, 75.80	2.64, 5.96	0.77, 2.68
(J) Benaras	70.83, 76.72	2.71, 5.91	0.78, 3.15
(K) Gwalior	70.70, 71.50	4.63, 6.09	1.35, 3.82
(L) Kangra	67.79, 55.58	4.68, 6.39	1.48, 3.19
(M) Srinagar	66.10, 63.50	4.73, 6.53	1.72, 2.82
(N) Jaipur	70.86, 69.42	2.94, 6.09	3.23, 1.38
(O) Bangalore	69.50, 81.20	3.45, 5.60	1.43, 4.17
(P) Pune	77.80, 74.50	3.73, 5.64	1.98, 10.63
(Q) Ahmedabad	70.67, 66.63	3.12, 6.13	3.37, 1.71
(R) Bhuj	70.48, 64.00	3.26, 6.04	3.92, 1.87
(S) Kathmandu	71.25, 72.50	2.69, 5.99	0.78, 2.87
(T) Bolpur	72.00, 78.40	3.19, 5.86	1.04, 2.72
(U) Hyderabad	80.17, 77.95	3.40, 5.68	1.15, 4.17

Day time $\beta = 0.3\ km^{-1}$ and h = 74 km; Night time $\beta = 0.38\ km^{-1}$ and h = 87 km; for all paths

each panel are put to mark the local sunrise and sunset times (see, Table 1).

In order to generally interpret the nature of the signals in winter, we plot in Fig. 4, the signal amplitude variation along the GCP from the transmitter to the receiving station using the very simple program of LWPC code which does not include solar flux variation at daytime. For the plotting purpose, we assume the day to be 25th of December. R marks the position of the receiver. The boxes are in the same sequence as given in Figs. 2, 3, i.e., (a) Imphal, (b) Agartala, (c) Salt Lake, (d) Malda, (e) Khukurdaha, (f) Kathmandu, (g) Hyderabad, (h) Gwalior, (i) Bangalore, (j) Pune, (k) Bhuj, and (l) Srinagar. Two curves are drawn in each box: C1 at 00:00:00 IST (solid) and C2 at 12:00:00 IST (dashed curve). If we first look at the box (i) (for Bangalore), we clearly see that C1 is stronger than C2 by about 10 dB at the receiver distance marked by 'R', which in general agreement with our observation. In Fig. 4c–e, we note that the midnight signals are stronger than the midday signals at the receiver's location as is observed. In Fig. 4h, the signals are comparable as also in Fig. 3h. In

Table 3 Summer campaign stations

Place	Latitude and longitude	Distance (km)	Sunrise (IST)	Sunset (IST)
Coochbehar	26°19′N, 89°28′E	2,347	04:52	18:25
Salt Lake	22°34′N, 88°24′E	1,963	05:03	18:22
Malda	25°00′N, 88°09′E	2,166	05:00	18:27
Raiganj	23°56′N, 88°08′E	2,207	04:59	18:28
Khukurdaha	22°27′N, 87°45′E	1,894	05:06	18:24
Bhagalpur	25°15′N, 87°01′E	2,117	05:04	18:32
Kathmandu	27°45′N, 85°20′E	2,296	05:06	18:44
Kangra	31°58′N, 76°40′E	2,625	05:32	19:27
Jaipur	26°55′N, 75°52′E	2,070	05:45	19:20
Srinagar	34°08′N, 74°51′E	2,867	05:34	19:39
Pune	18°34′N, 73°49′E	1,183	06:08	19:13
Bhuj	23°14′N, 69°40′E	1,863	06:17	19:38
Benaras	25°22′N, 83°00′E	1,948	05:20	18:49
Bolpur	23°40′N, 87°46′E	2,006	05:04	18:26

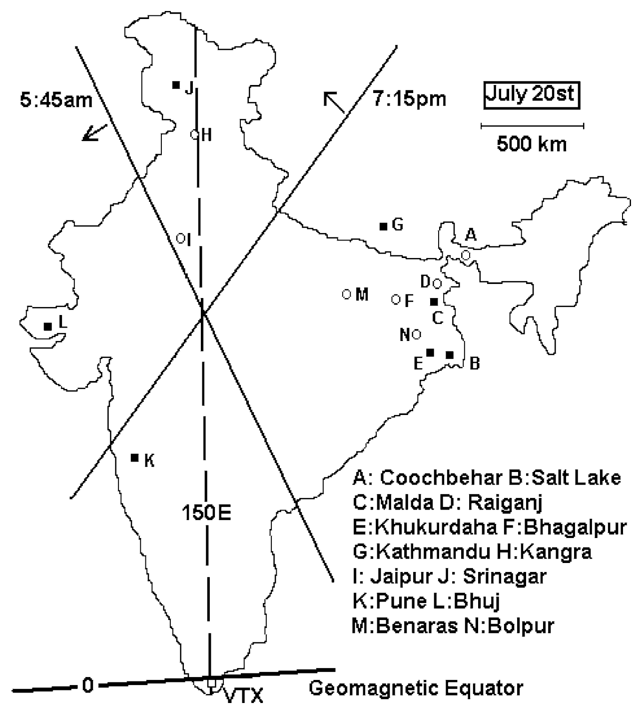

Fig. 6 The map of India showing all the receiving stations employed in our summer campaigns. Those shown by *filled squared boxes* are common to both summer and winter campaigns while those with *open circles* are only for the summer campaign. The geomagnetic equator and the magnetic longitude passing close to the VTX transmitter station are plotted for reference. The sunrise terminator and the sunset terminator at 5:30 am and 7:30 pm are shown to suggest how the signals would be influenced by the passage of the inclined terminators

Fig. 4g, j, k the midday signals are stronger at the receiver locations. Hence they also generally agree with observations. The Fig. 4l shows that from the Srinagar data one

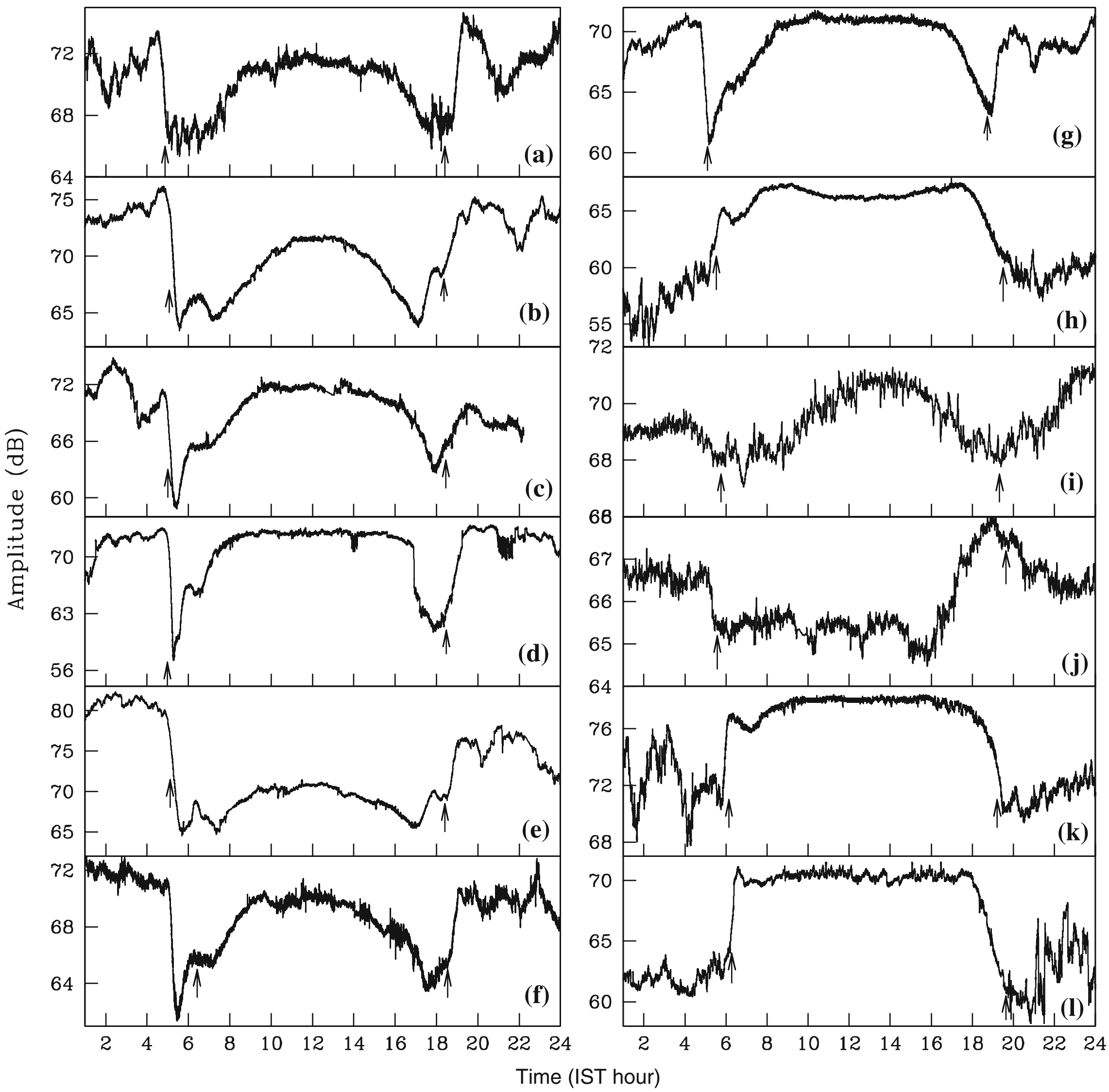

Fig. 7 Normalized observed data over the whole day in Indian Standard time (IST = UT + 5:30 h) from some of the receiving stations in summer: (*a*) Coochbehar (*b*) Salt Lake (*c*) Malda (*d*) Raiganj (*e*) Khukurdaha (*f*) Bhagalpur (*g*) Kathmandu (*h*) Kangra (*i*) Jaipur (*j*) Kashmir (*k*) Pune and (*l*) Bhuj. The data at (*a*–*g*) and (*i* and *j*) have strong night and weaker or comparable daytime signals. The data at (*h*), (*j* and *k*) have strong day time and weak night time signals

would also expect a W-type signal. However, we found the result to be very noisy and weak. Similarly results of Fig. 3a, b do not match with what is expected from Fig. 4a, b.

In Fig. 5, we present a rough nature of the diurnal signals expected from the LWPC code at each of the receiving stations. The signal amplitudes have been computed every hour at all the receiving stations. Near the terminator times when the D-layer is either forming (around 06:00 IST) or disappearing (around 18:00 IST) the computations were done every 5 min. It is clear that while the general shapes match, the details are missing in the LWPC results. In particular, the most prominent daytime feature, the effect of zenithal solar flux variation especially in the E-type signals are not seen here. The signals appear to be flat between the sunrise and the sunset. The signals at (a), (b), and (l) were not observed as expected. The data at (l) was noisy and is not shown.

As a summary of Figs. 4, 5, in Table 2, we present the predicted signal amplitudes at the midday, i.e., at 12:00 IST (06:30 UT) and at mid-night, i.e., at 00:00 IST (18.30 UT) at all the stations (summer and winter campaigns combined). We also present the attenuation rate of the 1st and the 2nd mode of propagation at the receiving points. Generally speaking, the attenuation rate of the 2nd mode is very high as compared to the first mode at the day time. At the night the attenuation is far less, but still the second mode attenuates faster. For Pune, which is about 1,200 km

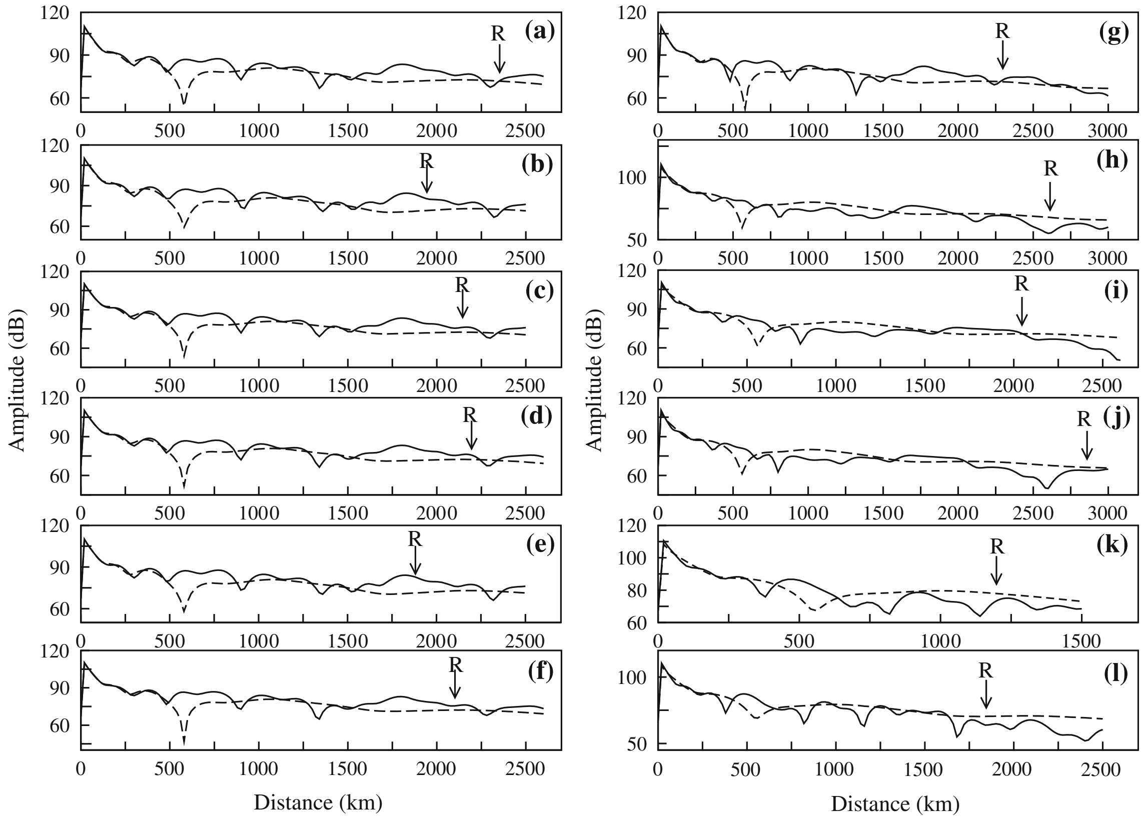

Fig. 8 The variation of the VLF signal amplitude as a function of the distance between the transmitter and the receiver as obtained from LWPC. For plotting purpose, we assume the day to be 20th July in the summer campaign. R marks the position of the receiver. The signals are for (*a*) Coochbehar, (*b*) Salt Lake, (*c*) Malda, (*d*) Raiganj, (*e*) Khukurdaha, (*f*) Bhagalpur, (*g*) Kathmandu, (*h*) Kangra, (*i*) Jaipur, (*j*) Kashmir, (*k*) Pune, and (*l*) Bhuj. The *curves* are drawn at 00:00:00 IST (*solid*) and 12:00:00 IST (*dashed*), respectively

away from the VTX station, the second mode attenuates about five times faster. Thus only the first mode is important in these stations.

4. Results from the summer campaign and interpretation

The campaign was conducted from the 20th to 27th of July, 2009. Table 3 shows the locations of the stations and their distances along the great circle path (GCP) from the transmitter. As before we also give the sunrise and sunset times. In Fig. 6, we show schematically the locations of the receiving stations. Out of the fourteen stations, nine were in the east and five were in west of the central meridian. We present the sunrise and sunset terminators on a typical day of the campaign at 5.45 am and 7.15 pm, respectively. Their directions of movements are shown with arrows. In Fig. 7, we present the received signals. The station are located at: (a) Coochbehar, (b) Salt Lake, (c) Malda, (d) Raiganj, (e) Khukurdaha, (f) Bhagalpur, (g) Kathmandu, (h) Kangra, (i) Jaipur, (j) Srinagar, (k) Pune, and (l) Bhuj (See also Fig. 6 for corresponding stations). Just as in the winter campaign, the signals seem to be of two types: The signals of (a–g) belong to E-type where the night time signals are strong and the daytime signals are weaker. As before, the day time signal follows the zenithal flux variation of the Sun. The W-type signal is observed at (h) and (k and l) where the day time signal is strong and the night time signal is attenuated. The daytime signal in this case is flatter (and often having opposite curvature as compared to the E-type signal) than what is expected from the diurnal solar flux variation. The signal at (i) is somewhat intermediate type having only $\sim$2 dB variation in 24 h. The signal obtained at Srinagar is also very weak and flatter in the day time with a total daily variation of only about 2 dB. As before, the arrows in each panel are put to mark the local sunrise and sunset times.

To understand the nature of signals along the bearings of each receivers, as well as to find the signal strengths at the receivers themselves, we show in Fig. 8, the signal amplitude variation along the GCPs from the transmitter to the receiving stations using the LWPC code. For the plotting purpose, we assume the day to be 20th of July. R marks the position of the receiver. The boxes are in the same sequence as given in Figs. 6, 7, i.e., (a) Coochbehar, (b) Salt Lake, (c) Malda,

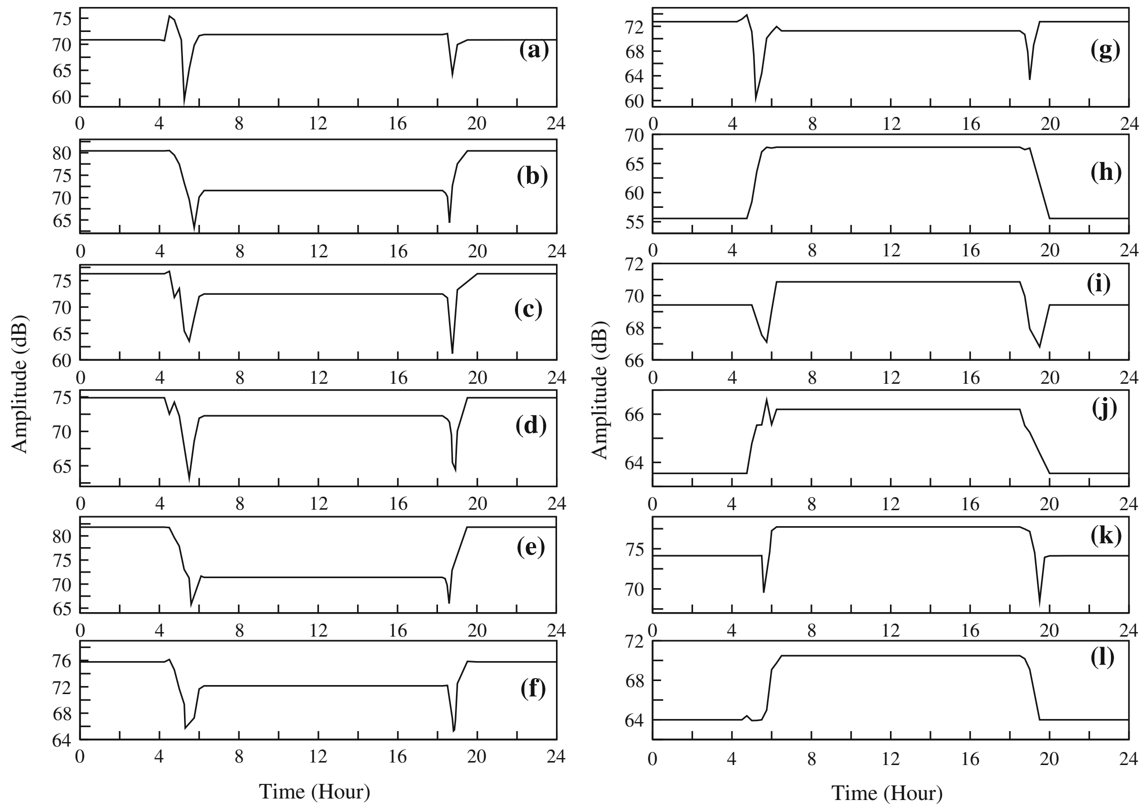

Fig. 9 The diurnal variation of the VLF signal amplitude at different receiving stations as obtained by LWPC in summer. The signals are for (*a*) Coochbehar, (*b*) Salt Lake, (*c*) Malda, (*d*) Raiganj, (*e*) Khukurdaha, (*f*) Bhagalpur, (*g*) Kathmandu, (*h*) Kangra, (*i*) Jaipur, (*j*) Kashmir, (*k*) Pune, (*l*) Bhuj. The results generally match with observations qualitatively, though the details are missing

(d) Raiganj, (e) Khukurdaha, (f) Bhagalpur, (g) Kathmandu, (h) Kangra, (i) Jaipur, (j) Srinagar, (k) Pune, and (l) Bhuj. Two curves are drawn in each box: C1 at 00:00:00 IST (solid) and C2 at 12:00:00 IST (dashed). For signals of (a–g) we find that indeed the midnight signals are either stronger or at least as strong as the noon signals. In cases of (h) and (k and l), the midnight signals are weaker compared to the noon signals. In the panel (j) the signals of C1 and C2 are comparable. The signal at panel (j) shows that the signals should be of similar strength in midday and midnight. We observe a very little variation in Fig. 7j.

As in winter campaign, in Fig. 9 we plot what the LWPC signals would look like at the receiving stations. The LWPC signals, while missing many details, do capture the salient features. We observe that signals at (a–g) are indeed E-type while the signals at (h–l) are W-type.

5. Comparison of the results and interpretations

In Fig. 10, we present a summary of the attenuation co-efficients in the first two modes of propagation during the daytime and nighttime propagations. The color bars represent the attenuation in units of the db/Mm. Contours of constant attenuation are superposed on the plot. Along the X-axis we present the bearing angle and along the Y-axis we present the distance from VTX station which is located at the origin of the plot. All the stations where receivers were kept are represented by filled circles (Table 2). The circles having smaller positive bearings are to the east of the geomagnetic meridian and those having larger bearings are to the west of the geomagnetic meridian. The top left and top right panels show attenuations of the first and the second modes at 12.00 IST. The bottom left and bottom right panels show attenuations of the first and second modes at 0.00 IST.

Finally, in Fig. 11, we compare the signals obtained at some of the common stations in winter and summer. The signals in panels (a–d) are E-type and those in panels (e–f) are W-type. The arrows mark the local sunrise and sunsets. The lengthening of the VLF-days between the terminators in the summer is understandable, particularly for those stations showing E-type signals. The signals were normalized to the midday value coming from LWPC code.

6. Discussions of the results and concluding remarks

In this paper, we have presented the results of VLF campaign with receiving stations spanning the whole of Indian sub-continent including Nepal, a region covering around 4 million

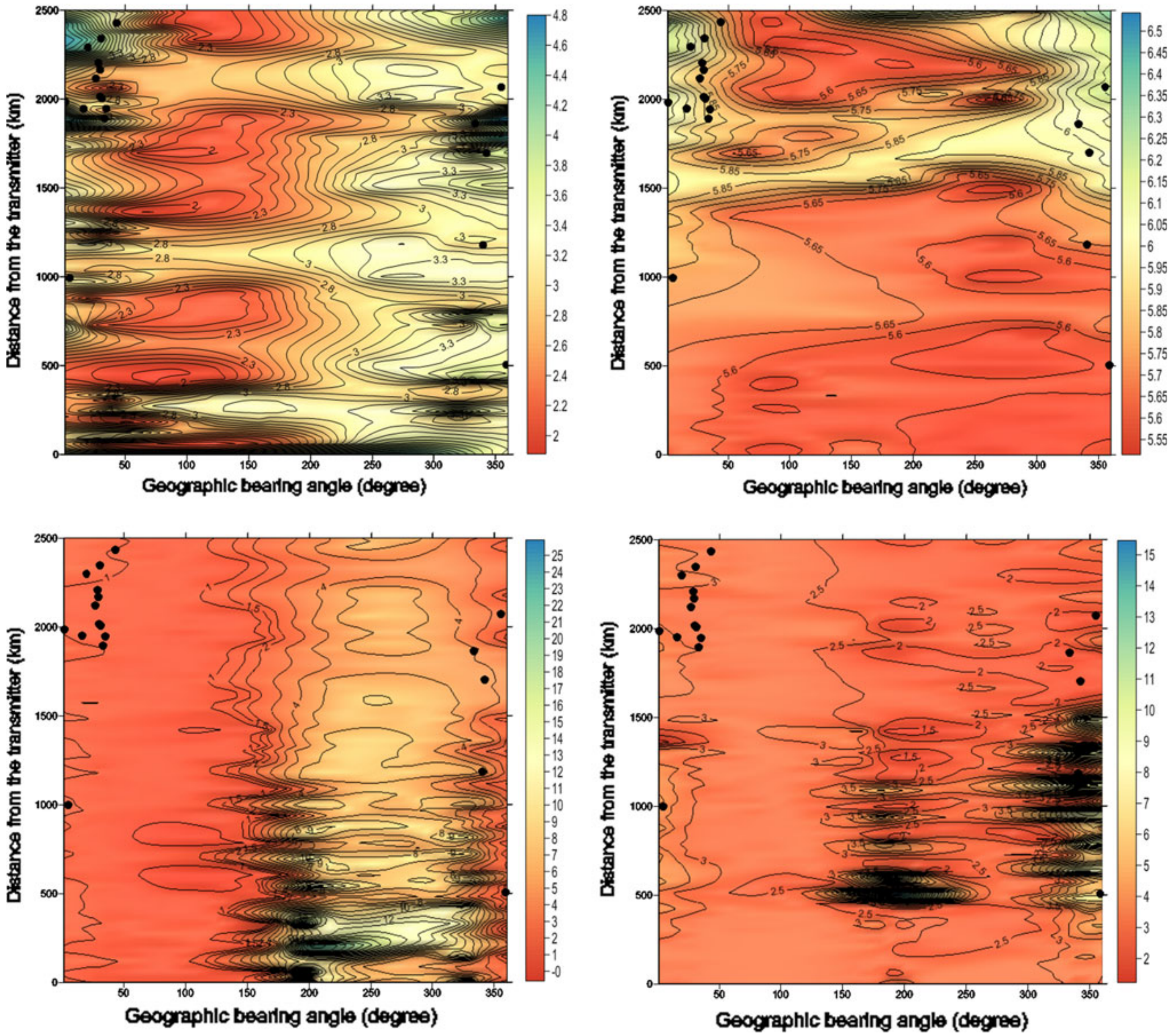

Fig. 10 Variation of the signal attenuations as a function of the bearing angle (X-axis) and distance from the transmitter (Y-axis). Superimposed are the contours of constant attenuation. VTX is located at the origin of this plot. The locations of all the stations are denoted by *filled circles*. **a** Mode 1 (daytime). **b** Mode 2 (daytime). **c** Mode 1 (nighttime). **d** Mode 2 (nighttime)

sq km. The unique location of the VTX station and the division of Indian subcontinent (geomagnetic meridian passing through VTX) by almost two equal parts makes it an ideal testbed for the existing theoretical models of propagation through the Earth-ionosphere waveguide. Indeed, from our data, we could easily distinguish two types of signals: In the east-type or E-type signal seen in the eastern side of the geomagnetic meridian, the day time amplitude is weaker compared to the night time amplitude while in the west-type or W-type signal seen in the western side, the day time amplitude is stronger compared to the night time amplitude. In between, the signal shows the transition from one to the other.

Using the LWPC code we have been able to generally interpret this variation among the receivers. In majority of the campaign locations, the average amplitude at night and day match with that given by LWPC code. However, the details, particularly the effect due to the diurnal solar flux variation are not captured properly. The E-type amplitude variations are formed when the signal propagates from the west to the east, while the W-type signals are found to form when the signal propagates from the east to the west. Since the magnetic field is included in LWPC, the effect is caused by the switching of the sign of the magnetic field with respect to the propagation direction [12–14]. The regions close to the magnetic meridian

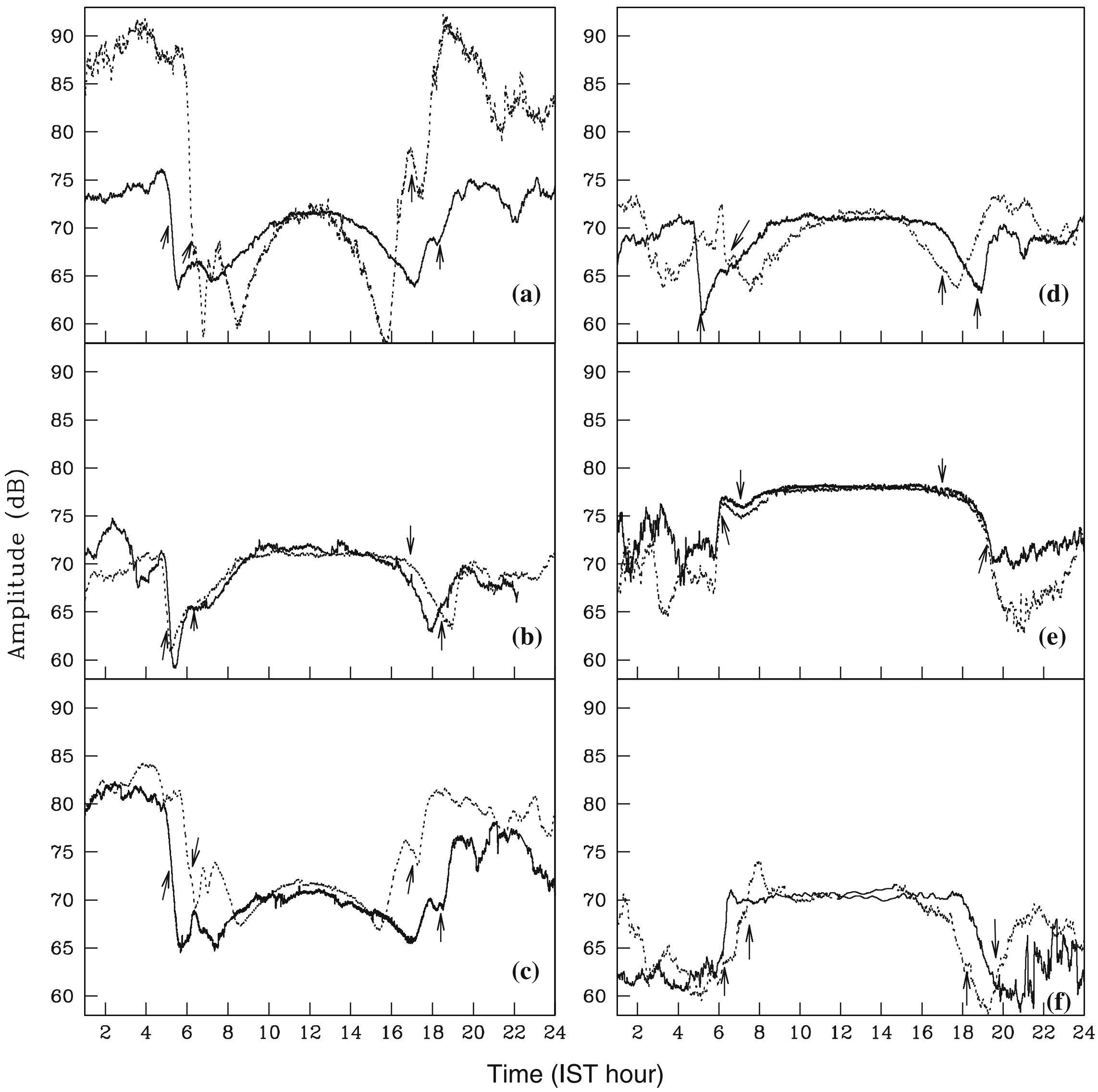

Fig. 11 The diurnal VTX signals at six common stations in summer (*solid curve*) and winter (*dashed curve*) campaigns are shown in order to highlight seasonal variations. Normalization has been done using the LWPC amplitude at 12 noon for comparison purpose only. The receiving stations are at: (*a*) Salt Lake, (*b*) Malda, (*c*) Khukurdaha, (d) Kathmandu, (*e*) Pune, and (*f*) Bhuj

of the transmitter show intermediate behavior and show similar night and daytime amplitude as the magnetic field perpendicular to the direction of propagation is negligible. The day time data of Bangalore is very weak and perhaps because it is very close to the skip distance.

From the campaign results and interpolation of them gives us a VLF map of Indian subcontinent *vis-a-vis* the VTX station which may be used as a template. Deviations from these templates can be used to obtain the properties of the ionospheric disturbances both by extraterrestrial (e.g., solar flares, gamma ray bursts, soft gamma ray repeaters, etc.) or terrestrial effects (e.g., lightning, earthquakes, etc.). During solar flares or GRBs and SGRs, the signal amplitude rises and the deviation throughout India could be computed from the templates. This would give us the nature of the ionospheric weather after such events [17–22]. The earthquake predictions depend on the details of the template (see, [23–26] and references therein). Similarly, in the case of solar eclipse, there will location dependent deviation of the signal [27–29]. A global ionospheric weather map can be made based on these studies from a large number of VLF weather stations.

Acknowledgments The authors thank Ram C Das, Somnath Midya, Partha S Pal, Chandra B Singh, Dilip D Joshi, M Thakkar, and S Mandal for helping at various stages to procure the data. They also thank D Sulic with the LWPC code. The research work of S K

Mondal was supported by CSIR grant. The research works of S Sasmal and S Ray are supported by RESPOND project of ISRO.

References

[1] S K Chakrabarti, S Pal, K Acharyya, S Mandal, S Chakrabarti, R Khan and B Bose *Indian. J. Phys.* **76B** 693 (2002)

[2] S K Chakrabarti, K Acharyya, B Bose, S Mandal, A Chatterjee, N M Nandi, S Pal and R Khan *Indian. J. Phys.* **77B** 173 (2003)

[3] M Altaf, K K Singh, S A Sheikh, A K Singh and Lalmani *Indian. J. Phys.* **84** 1481 (2010)

[4] P Pal, A Bhowmik, R Roy, R Ali, A Choudhury, A Guha and B K Dey *Indian. J. Phys.* **84** 641 (2010)

[5] L A Berry, *Radio Science J. Res.* **68D,** 1275 (1964)

[6] L A Berry and M E Chrisman *Radio Science J. Res.* **69** 1469 (1965)

[7] J R Wait *J. Geophys. Res.* **67** 3823 (1962)

[8] J R Wait *Rev. Geophys. Space. Phys.* **1** 481 (1963)

[9] J A Ferguson *Tech. doc. 3030, Space and Naval Warfare Systems Center, San Diego* (1998)

[10] J R Wait and K P Spies *NBS Tech. Note U.S. 300* (1964)

[11] K G Budden *Phil. Mag.* **42** 833 (1951)

[12] D D Crombie *J. Atmos. Terr. Phys.* **12** 110 (1958)

[13] D D Crombie *J. Res. Natl. Bur. Stand.* **65** 455 (1961)

[14] N F Barber and D D Crombie, *J. Atmos. Terr. Phys.* **16** 37 (1959)

[15] M Hayakawa, O A Molchanov, T Ondoh and E Kawai *J. Comm. Res. Lab. Tokyo* **43** 169 (1996)

[16] S Ray, S K Chakrabarti and S Sasmal *Indian. J. Phys.* **86** 85 (2012)

[17] U S Inan, N G Lehtinen, S J Lev-Tov, M P Johnson, T F Bell and K Hurley Geophys. Res. Lett. **26** 3357 (1999)

[18] S K Chakrabarti, S K Mondal, S Sasmal, D Bhowmick, A K Choudhury and N P Patra *Indian J. Phys.* **84** 1461 (2010)

[19] T Basak, S K Chakrabarti and S. Pal *Propagation Effects of Very Low Frequency Radio Waves* (ed.) S K Chakrabarti, *AIP Proceedings No.* 1286 (New York) p 137 (2010)

[20] S K Mondal and S K Chakrabarti *Propagation Effects of Very Low Frequency Radio Waves* (ed.) S K Chakrabarti, *AIP Proceedings No*. 1286 (New York) p 311 (2010)

[21] S K Mitra, *The Upper Atmosphere*, Royal Asiatic Society of Bengal (1943)

[22] A P Mitra and J N Rowe *J Atmos Terr Phys*, **34** 795 (1972)

[23] S Sasmal, S K Chakrabarti and S Chakrabarti, *Propagation Effects of Very Low Frequency Radio Waves (*ed.) S K Chakrabarti, AIP Proceedings No. 1286 (New York) p 270 (2010)

[24] S Sasmal and S K Chakrabarti *Nat. Hazards. Earth. Syst. Sci.* **9**, 1403 (2009)

[25] S Ray, S K Chakrabarti and S Sasmal *Nat. Hazards. Earth. Syst. Sci.* **11**, 2699 (2011)

[26] S K Chakrabarti, S Sasmal and S Chakrabarti *Nat. Hazards. Earth. Syst. Sci.* **10**, 1751 (2010)

[27] S K Chakrabarti, S Pal, S Sasmal, S K Mondal, S Ray, T Basak, S K Maji, B Khadka, D Bhowmick and A K Chowdhury *J. Atmos. Sol. Terres. Phys.* (to appear) (2012)

[28] S K Maji, S K Chakrabarti and S K Mondal *Propagation Effects of Very Low Frequency Radio Waves* (ed.) S K Chakrabarti, *AIP Proceedings No.* 1286 (New York) p 214 (2010)

[29] S K Maji, S K Chakrabarti and S K Mondal *Earth, Moon and Planets* (in press) (2012)